Bitlis Eren Üniversitesi Fen Bilimleri Dergisi
BİTLİS EREN UNIVERSITY JOURNAL OF SCIENCE
ISSN: 2147-3129/e-ISSN: 2147-3188
VOLUME:11 NO: 2 PAGE: 666-677 YEAR: 2022
DOI: 10.17798/bitlisfen.1080973

Stress-Controlled Dynamic Triaxial Experiments to Examine the Liquefaction Response of Clean Sand

Abdülhakim ZEYBEK[1*]

[1]*Muş Alparslan University, Faculty of Engineering-Architecture, Department of Architecture, Muş (ORCID: 0000-0001-7096-5770)*

Keywords: Dynamic triaxial testing, Stress-controlled tests, Liquefaction, Clean sand.

Abstract

Loosely packed cohesionless soils may suffer partial or complete liquefaction during seismic loading, causing significant structural damage. The dynamic behavior of liquefiable soils is widely investigated through element testing under controlled cyclic loading in undrained conditions. In this work, a total of 20 stress-controlled dynamic triaxial experiments were conducted to investigate the influence of loading frequency and relative density on the liquefaction behavior of clean sand. The triaxial specimens were prepared at different relative densities in the range of 38 to 90% and subjected to varying cyclic stress ratios (CSR) with loading frequencies of 0.1 and/or 1 Hz. The experimental results indicated that under similar test conditions, the number of cycles needed for liquefaction was greater at 1 Hz than at 0.1 Hz, revealing that sand specimens exhibited higher liquefaction strength at higher loading frequencies. Furthermore, regardless of the cyclic loading frequency, the liquefaction resistance of sand increased with increasing densities.

1. Introduction

Historical records indicate that soil liquefaction resulted in significant damage in many past earthquake events [1]. Extensive liquefaction-induced deformations (i.e., sand boils, landslides, lateral spreading, bridge, and shallow foundation failure) were observed in the 1964 Alaska-USA earthquake [2] and the Niigata-Japan earthquake [3], which captivated the interest of researchers and engineers. Since the 1964 earthquakes, a concentrated research effort has been devoted to liquefaction-related problems, and these studies have provided important knowledge on different aspects of earthquake-induced liquefaction [4], [5]. Despite remarkable advances over the last half-century, a complete understanding of the liquefaction phenomenon remains incomplete due to its complex nature, and there are still some uncertainties regarding the influencing parameters. Earthquake-induced liquefaction is still threatening the safety of structures all around the world, and this fact underlines the need for further study on this topic.

Some researchers constructed fully instrumented sites to capture the in situ soil behavior during an earthquake event [6]. Although real earthquake data is ideal to correctly evaluate the in situ behavior of liquefiable soil, it is extremely challenging and economically unfeasible in many cases. Therefore, many researchers have concentrated on alternative research methodologies (i.e., physical modeling, and element testing). Amongst these, element testing (i.e., dynamic triaxial, cyclic simple shear tests) has become more popular and commonly used by geotechnical engineers as it allows studying the problem of liquefaction under controlled and repeatable test conditions, and its cost is comparatively lower.

Liquefaction is directly related to excess pore pressures developed under seismic loading, which causes substantial effective stress and shear stiffness degradation. Seed and Lee [7] performed cyclic triaxial experiments on clean sand specimens and proposed the condition of initial liquefaction in which excess pore pressures (u_e) develop and become equal to initial effective confining stress (σ_o' or σ_c'). It was

*Corresponding author: a.zeybek@alparslan.edu.tr
Received: 05.03.2022, Accepted: 21.04.2022

shown that loose sand samples suffered complete liquefaction because of the quick build-up of excess pore pressures and extensive shear strength degradation occurred over a large amplitude of strains, whereas dense samples suffered gradual softening and dilated at large strains. Ishihara [8] later proposed that a 5% double amplitude axial strain that occurred during undrained cyclic loading corresponds to the onset of liquefaction. Muhunthan and Schofield [9] suggested that besides the state of zero effective stress, the formation of cracks or micro-fissures, and high hydraulic gradients are crucial for the occurrence of liquefaction.

Liquefaction studies reveal that relative density (D_r), initial effective confining stress (σ_c'), and fines content (FC) are some of the important parameters that govern the cyclic response of liquefiable soils. Considering the field observations from the 1964 Niigata earthquake, the main focus of the earlier studies was placed on sandy soils [10], [11]. However, following numerous field observations that sands with some amount of silt and/or clay and silt can also liquefy when subjected to seismic loading, many researchers have extended their interest in elucidating the role of fines in the response of sandy soils. These studies concluded that the type and plasticity of fines and fine content were important factors influencing the liquefaction behavior of sand-silt or sand-clay mixtures [12]-[17]. The analysis of case histories and experimental studies provided conclusive evidence that loose deposits of sandy soils suffer larger volumetric compaction during cyclic loading, generating higher excess pore pressures. The tendency for volumetric strains significantly decreases as relative density increases. Researchers reached a consensus that increasing the relative density of sandy soils enhances the liquefaction resistance [18]-[21]. Through extensive laboratory studies, researchers also reached an agreement that initial effective confining stress significantly affects the liquefaction resistance of sandy soils, which reduces as confining stress increases [22]. This effect was observed to be particularly more noticeable at larger densities.

It is known that real earthquakes involve irregular shear stresses and the frequency content of seismic excitation varies (typically 0-15 Hz). Through the cyclic laboratory tests, investigators have suggested that the liquefaction behavior of sandy soils relies not only on the initial test conditions but also on the frequency of seismic loading. Due to the experimental difficulties and inherent limitations of the test devices, many of these studies have been conducted using sinusoidal loading. Some early studies showed that loading frequency has an insignificant impact on the soil's liquefaction behavior [23]-[26]. More recent studies have reported that an increase in loading frequency leads to an increase in liquefaction resistance of sandy soils [27]-[32]. On the contrary, some researchers have observed higher liquefaction resistance at lower loading frequencies [33], [34]. From this review of literature, it is obvious that, despite a large number of studies, no common consensus has been reached, and the effect of loading frequency remains unclear. Further study of this topic will be of value to draw more definite conclusions.

The current study aims to offer valuable insights into the impact of loading frequency and relative density on the cyclic behavior of liquefiable soils. With this aim, several stress-controlled dynamic triaxial experiments were conducted on clean sand from the Sile region of Istanbul. The reconstituted triaxial specimens were prepared with different relative densities ranging from 38 to 90%, and were tested under undrained cyclic loading conditions with varying cyclic stress ratios at two different loading frequencies (0.1 and 1 Hz).

2. Experimental Investigation

2.1. Materials Tested

In this work, triaxial specimens were prepared using clean silica sand (AFS 55/60). The sand was taken from a sand quarry located in the Sile-Istanbul region. Figure 1 demonstrates the particle size distribution (PSD) determined through the dry sieve analysis. Table 1 summarizes the main physical properties obtained in general accordance with ASTM standards. As per the United Soil Classification System (USCS), this type of soil is poorly graded sand (SP).

In the aftermath of the 1964 earthquakes, extensive laboratory research has been conducted on specimens of clean sand obtained from various quarries around the world. Due to their wide availability, some of the test materials (i.e., Ottawa, Toyoura, Nevada, Monterey, Hostun sand) have been highly preferred by researchers, and thus the liquefaction behavior of these sands has been firmly established in geotechnical earthquake engineering. Alternatively, due to the increased cost of imported sand, many researchers tend to use locally available soils. The grain size distribution analysis offers useful insights into the suitability of local sands for liquefaction studies. Figure 1 compares the PSD of Sile sand with the liquefaction boundaries recommended by Tsuchida [35]. It appears that Sile sand falls into the boundaries of most liquefiable soil.

It is highly liquefaction susceptible soil and suitable material for liquefaction studies [36], [37].

Table 1. Basic physical properties of sand used in this study

Properties	Value
Median particle size, D_{50} [mm]	0.296
Coefficient of uniformity, C_u	1.352
Specific gravity, G_s	2.65
Min. void ratio, e_{min}	0.574
Max. void ratio, e_{max}	0.885
USCS classification	SP

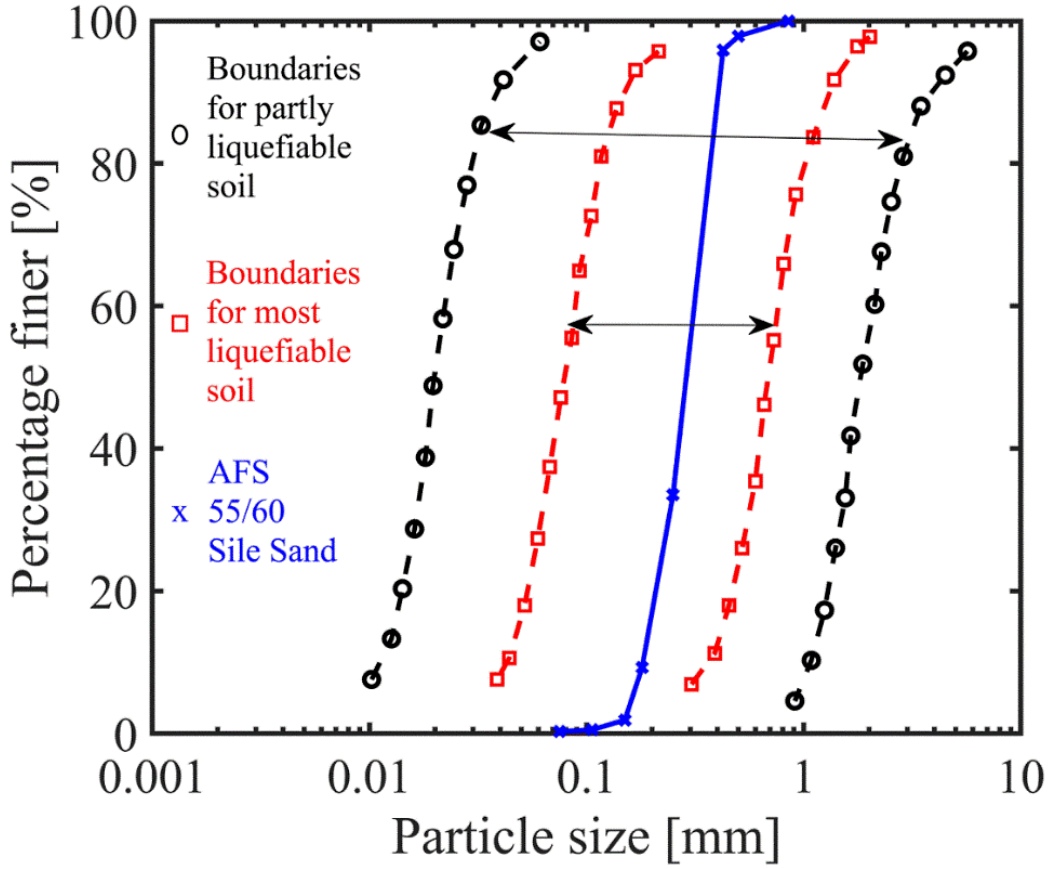

Figure 1. Particle size distribution curve for AFS 55/60 Sile sand

2.2. Testing Apparatus

The experiments were conducted using the Dynatriax EmS apparatus located in the Civil Engineering Laboratory of Mus Alparslan University. Figure 2 shows the main components of the test system.

The Dynatriax EmS system is manufactured by Wykeham Farrance-Controls Groups. It is a fully automated electromechanical apparatus that can conduct stress and/or strain-controlled dynamic triaxial experiments in drained and undrained conditions. The apparatus has a dynamic actuator that can apply loading cycles in the range of 0.01-10 Hz.

During the experiments, saturation, consolidation, and cyclic loading of triaxial specimens were automatically controlled with the assistance of the Dynatriax software and data acquisition system. The saturation of specimens was assessed by checking Skempton's B value. Once the cyclic loading ceased, the excess pore pressure dissipation was performed with the solenoid valve located on the drainage line. The cell, back and excess pore water pressures, axial load/displacements, and volume changes were measured through the monitoring sensors, including pressure transducers, submersible load cell, linear variable differential transducers, and an automatic volume change device. The instruments were periodically calibrated.

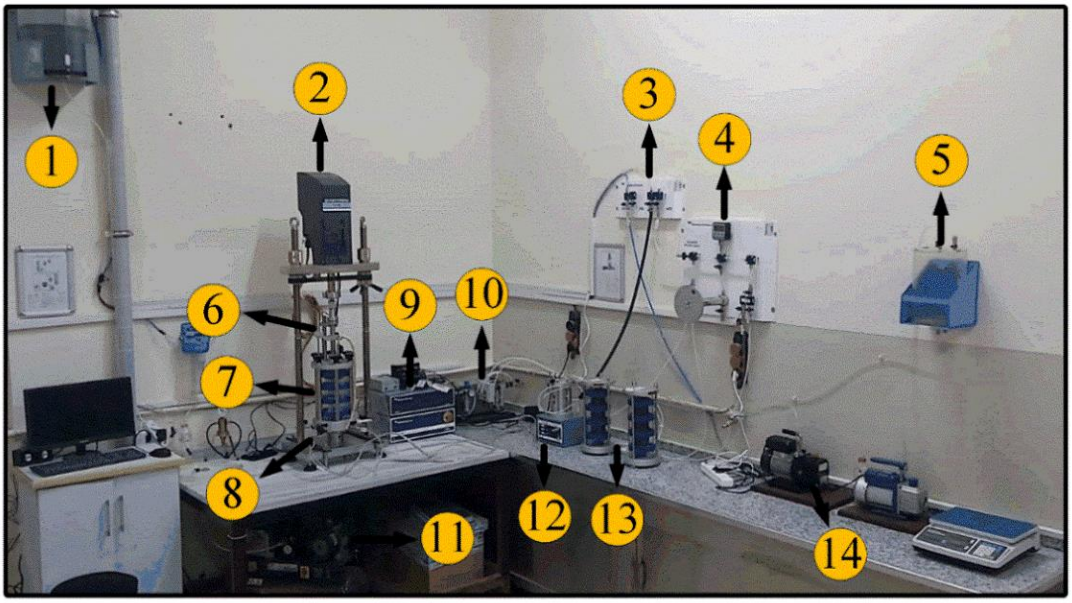

1) De-airing tank, 2) Actuator, 3) Valve panel, 4) Water distribution panel, 5) Vacuum chamber, 6) LVDT, 7) Triaxial cell and submersible load cell, 8) Pressure transducer, 9) CDC and Drive unit, 9) Air receiver, 10) Air compressor, 11) Volume change device, 12) Air/water cylinders, 13) Vacuum pumps

Figure 2. The main components of the dynamic triaxial system used during the experimental work

2.3. Testing Procedure

2.3.1. Preparation of Sand Specimens

The loose ($D_r \approx 40\%$) and medium dense specimens ($D_r \approx 55\%$) were prepared using the dry pluviation technique, while dense specimens ($D_r \approx 90\%$) were prepared using the dry tamping method. The diameter (D) of the reconstituted sand specimens was 70 mm, and the ratio of height to diameter (H/D) was approximately 2 during the tests. Figure 3 shows different stages of specimen preparation.

After flushing the drainage lines with de-aired water, a porous stone, filter paper, and latex membrane were placed over the base pedestal of the triaxial cell. This was followed by the placement of a cylindrical split mold (Figure 3a). For loose to medium dense specimens, the sand was rained into the mold utilizing a modified funnel with a sieve and maintaining a constant drop height. The opening sizes of the sieve were varied to adjust the density. For the dense specimens, sand was compacted in 10 equal layers by freely dropping a tamper from a predetermined height. The top cap, filter paper, and porous stone were positioned (Figure 3b). Vacuum pressure (20 kPa) was applied before removing the split mold, maintaining the verticality of the sand specimens (Figure 3c). The specimen heights were measured with caution.

The triaxial cell was mounted and then filled with de-aired water. Eventually, 20 kPa cell pressure was applied before the suction was released (Figure 3d).

2.3.2. Saturation, Consolidation, and Shearing of Sand Specimens

On completion of specimen preparation, the sand specimens were saturated, consolidated, and subjected to cyclic loading. Figure 4 presents a schematic of the stages of the dynamic triaxial tests.

The specimens were washed with carbon dioxide gas (CO_2) and de-aired water to expedite the saturation process. CO_2 gas was carefully applied to the specimens, giving special attention to gas pressure that remained within desirable limits (typically 10 kPa). After 20 minutes of CO_2 flushing, de-aired water was passed through the sand specimens. This was followed by a cell and back pressure ramp involving a gradual increase in cell pressure (CP or σ_3) and back pressure (BP or u_0) by maintaining a constant differential pressure ($\sigma_c' = 10$ kPa). This process ceased once the desired back pressure (u_0 =350 kPa) was accomplished. The Skempton's coefficient ($B = \frac{\Delta_u}{\Delta\sigma_3}$, where Δ_u and $\Delta\sigma_3$ correspond to pore pressure and confining stress change, respectively) was periodically measured to control the status of saturation, and the B values at the beginning of the consolidation process were ranging from 0.99 to 1.

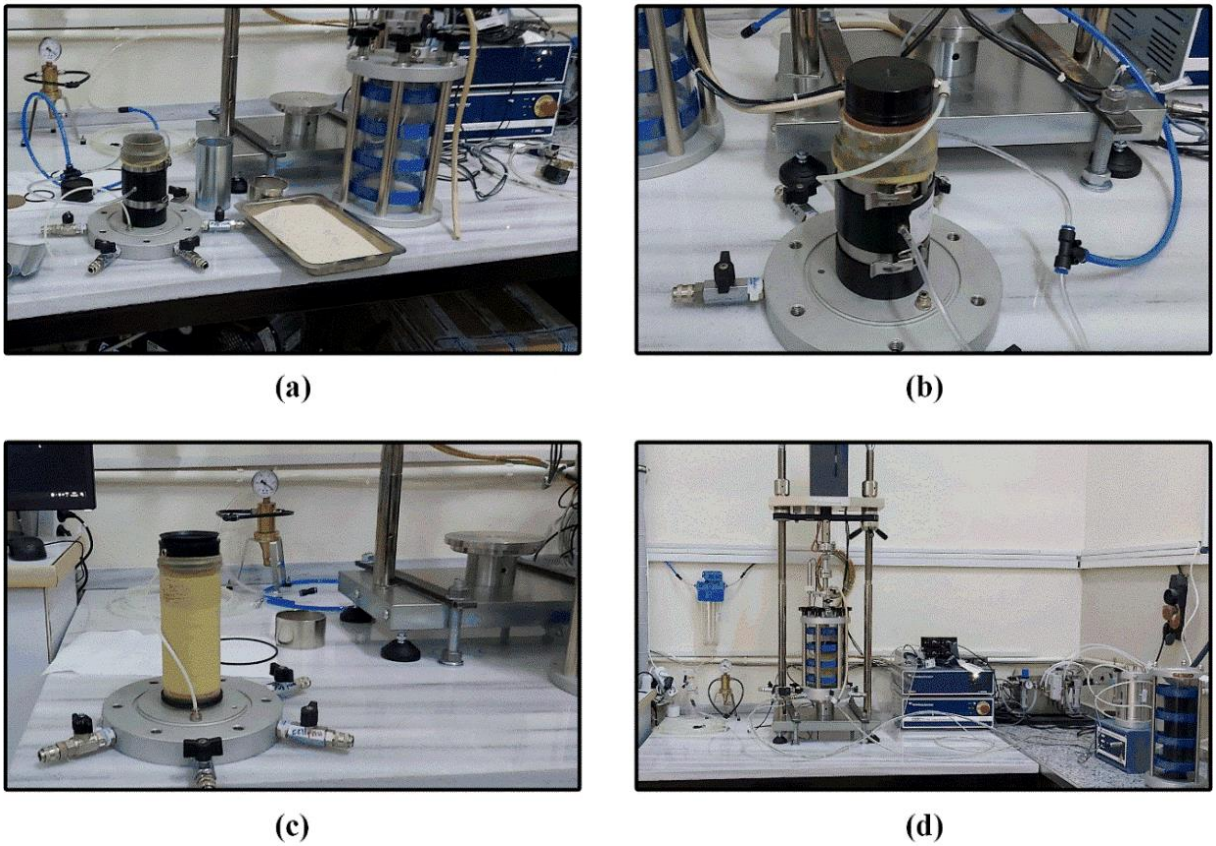

Figure 3. Preparation of triaxial specimens

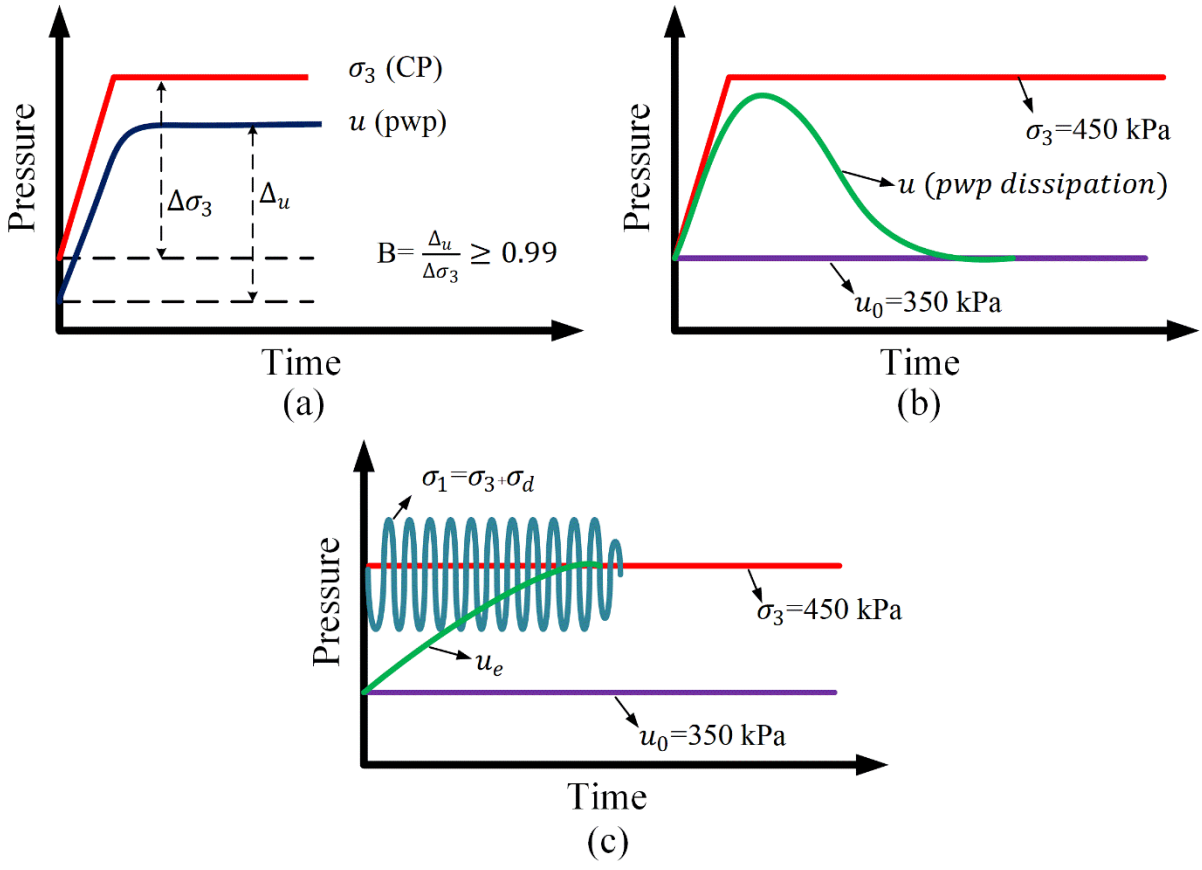

Figure 4. Saturation, consolidation, and cyclic loading of triaxial specimens

Saturated specimens were isotropically consolidated to 100 kPa ($\sigma_c' = 100$ kPa) by maintaining the back pressure at 350 kPa and increasing the cell pressure up to 450 kPa. At the end of the consolidation process, where volume changes were insignificant, the specimens were subjected to a simple harmonic (sinusoidal) loading.

A total of 20 stress-controlled dynamic triaxial experiments were carried out in undrained conditions. Table 2 gives a summary of the test program and provides typical experimental results that are representative of a larger database. The reconstituted specimens at loose, medium, and dense conditions were axially loaded at different amplitudes of cyclic stress, having two different loading frequencies, which are the most widely used in stress-controlled dynamic triaxial tests, namely 0.1 and 1 Hz. The applied cyclic stress ratios ($CSR = \frac{\sigma_d}{2\sigma_c'}$, where σ_d and σ_c' denote the deviatoric stress and effective confining stress, respectively) ranged from 0.08 to 0.3.

Table 2. Experimental program and typical test results

Test No	Test ID	Specimen Density	D_r (%)	u_0 (kPa)	σ_c' (kPa)	Frequency (Hz)	CSR	N_{liq}
1	LS1		40.0	350	100	0.1	0.08	194
2	LS2		39.0	350	100	0.1	0.10	75
3	LS3		38.0	350	100	0.1	0.13	23
4	LS4	Loose Sand	41.0	350	100	0.1	0.18	3
5	LS5		42.0	350	100	1.0	0.08	220
6	LS6		39.0	350	100	1.0	0.10	83
7	LS7		40.0	350	100	1.0	0.13	33
8	LS8		39.0	350	100	1.0	0.18	3
9	MS1		55.0	350	100	1.0	0.13	581
10	MS2	Medium	56.0	350	100	1.0	0.18	57
11	MS3	Dense Sand	55.0	350	100	1.0	0.20	27
12	MS4		54.0	350	100	1.0	0.25	1
13	DS1		89.0	350	100	0.1	0.18	670
14	DS2		88.0	350	100	0.1	0.23	102
15	DS3		88.0	350	100	0.1	0.26	35
16	DS4	Dense Sand	87.0	350	100	0.1	0.30	1
17	DS5		90.0	350	100	1.0	0.18	791
18	DS6		88.0	350	100	1.0	0.23	121
19	DS7		87.0	350	100	1.0	0.26	43
20	DS8		89.0	350	100	1.0	0.30	2

3. Results and Discussions

3.1. Behavior of Clean Sand under Undrained Cyclic Loading

Figure 5 presents typical experimental results for loose and dense specimens. The specimens having a relative density (D_r) of 41 and 88% were tested under deviatoric stress (q) of 36 kPa and 52 kPa at initial effective confining stress (σ_c') of 100 kPa, corresponding to cyclic stress ratios of 0.18 and 0.26.

It can be inferred from the figure that regardless of relative density, significant excess pore pressures (u_e) accumulated during undrained cyclic loading and caused significant effective stress and stiffness degradation. The rate of excess pore pressure accumulation was different for the loose and dense specimens. The loose sand specimen suffered a rapid development of excess pore pressure. After a few loading cycles, pore pressure reached the initial confining (total) stress, and the excess pore pressure ratio (r_u) was equal to unity, corresponding to the initiation of liquefaction. Mean effective stress (p') reduced with increasing excess pore pressure, and the stress path moved towards the critical state line, showing a flow type behavior.

In the dense sand specimen, the first cycle caused a rapid increase of excess pore pressure and a rapid reduction of p'. During the following cycles, excess pore pressure increased progressively, and the decrease in p' was more gradual. The stress path touched the critical state line after a larger number of loading cycles. The observed trends are valid for the simple harmonic loading condition and structures of sand created with reconstitution methods of dry pluviation and tamping methods.

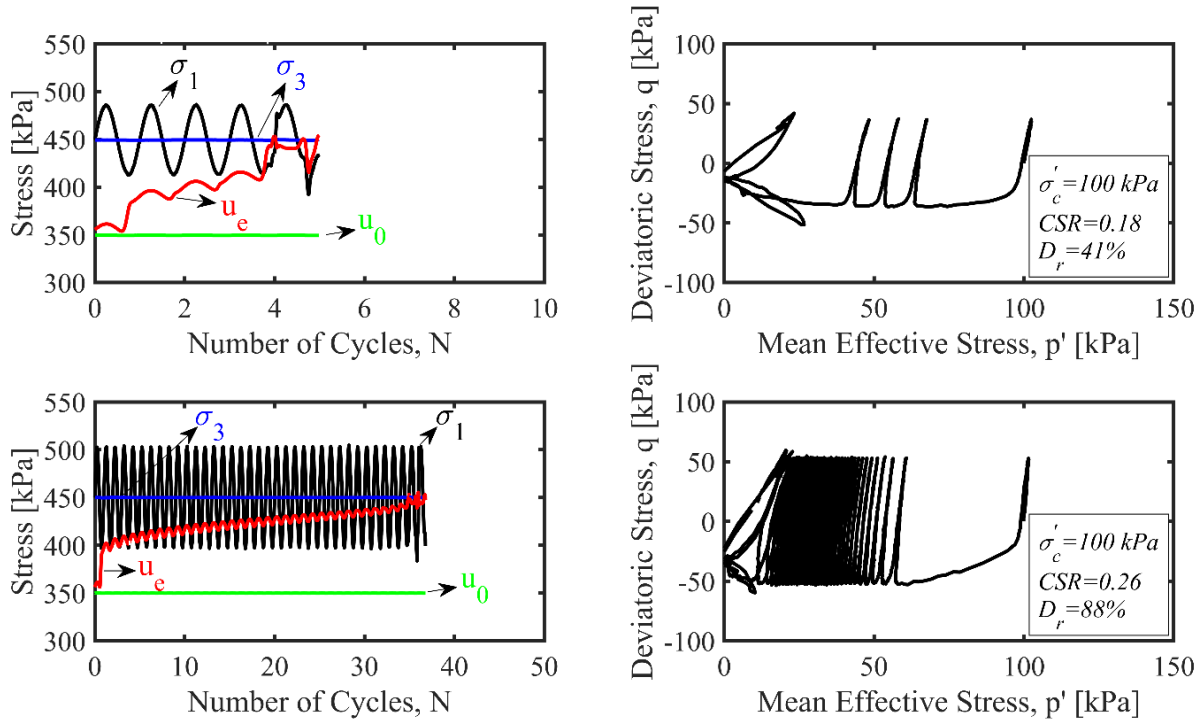

Figure 5. Typical cyclic behavior of sand specimen under undrained loading condition

3.2. Excess Pore Pressure Development

Experimental data recorded at different relative densities and loading frequencies are presented in this section to discuss the role of density and frequency in the development of excess pore pressure. For this purpose, excess pore pressure ratios (r_u) are plotted against the number of cycles (N).

Figure 6 illustrates the r_u – N plots for loose, medium, and dense sand specimens tested at the same loading frequency and σ_c'. It is clear that under the same cyclic stress ratio ($CSR = 0.18$), the loose sand specimen ($D_r = 39\%$) showed a faster excess pore pressure development, causing a significant reduction in sand's stiffness and extensive soil softening.

The liquefaction criterion ($r_u = 1$) was satisfied after approximately three loading cycles. In medium dense sand ($D_r = 56\%$), excess pore pressure seems to grow relatively slowly, and sand liquefied after the application of 57 loading cycles. It seems that softening was intensified when r_u was in the vicinity of 0.70. The excess pore pressure accumulated in the dense sand was very small at 100 loading cycles, and a significant number of loading cycles were required for $r_u = 1$. The medium dense sand was observed to behave like loose sand when subjected to CSR of 0.25-0.26. The results also exhibit that dense sand liquefied when the magnitude and number of applied cyclic stresses were sufficient enough to cause liquefaction.

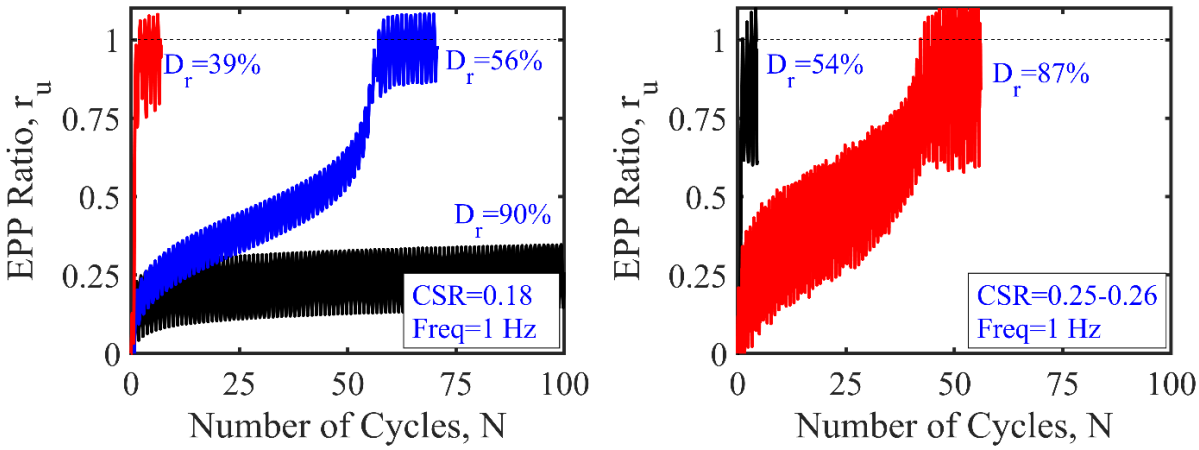

Figure 6. Typical excess pore pressure data recorded at different relative densities

Figure 7 plots the excess pore pressures captured at 0.1 and 1 Hz to provide insights into the influence of loading frequency. This analysis was conducted for loose and dense specimens tested at CSR of 0.08 and 0.23, respectively. The results exhibited that excess pore pressures increased in both cases, and ultimately reached σ_c'=100 kPa. Under analogous test conditions, the number of cycles required for liquefaction was larger at a higher loading frequency (1 Hz) than at a lower frequency (0.1 Hz). The interesting observation is that for both loose and dense sand the build-up of excess pore pressure was faster during the initial cycles, and it accumulated at a slower rate in the subsequent cycles. Moreover, for the density ranges under consideration, the rise of excess pore pressure at the early stages of the cyclic loading was faster at 0.1 Hz than at 1 Hz.

3.3. Liquefaction Resistance

The above results emphasized the role that relative density and loading frequency play in the excess pore pressure response of Sile sand. To offer further insights into this matter, cyclic resistance curves, presenting the relationship between the cyclic stress ratio (CSR) and the number of cycles for liquefaction N_{liq}, are depicted in Figures 8 and 9.

Figure 8 provides information about the influence of relative density on sand's liquefaction resistance. Regardless of the loading frequency, dense sand required much higher CSR than loose sand at the same number of cyclic loadings. This indicated that sand specimens exhibit a much higher liquefaction resistance as the density increased, as expected. This finding appears to be consistent with the results of many published studies [18]-[21].

N_{liq} values recorded during 1 Hz tests were normalized with those measured during 0.1 Hz tests. Figure 9 depicts the variation of normalized N_{liq} with CSR for loose and dense sand. In almost every test, the resistance of sand to liquefaction was much higher at 1 Hz. Irrespective of D_r and CSR, the liquefaction resistance of loose and dense sand was observed to increase as the loading frequency increased from 0.1 to 1 Hz. These observations are in agreement with many previous research studies [27]-[32]. The experiments carried out at the same CSR showed that the effect of loading frequency was more noticeable for dense sand than loose sand. It is noteworthy that this observation was made based on a limited dataset, and further research will be useful to draw a more concrete conclusion about this aspect.

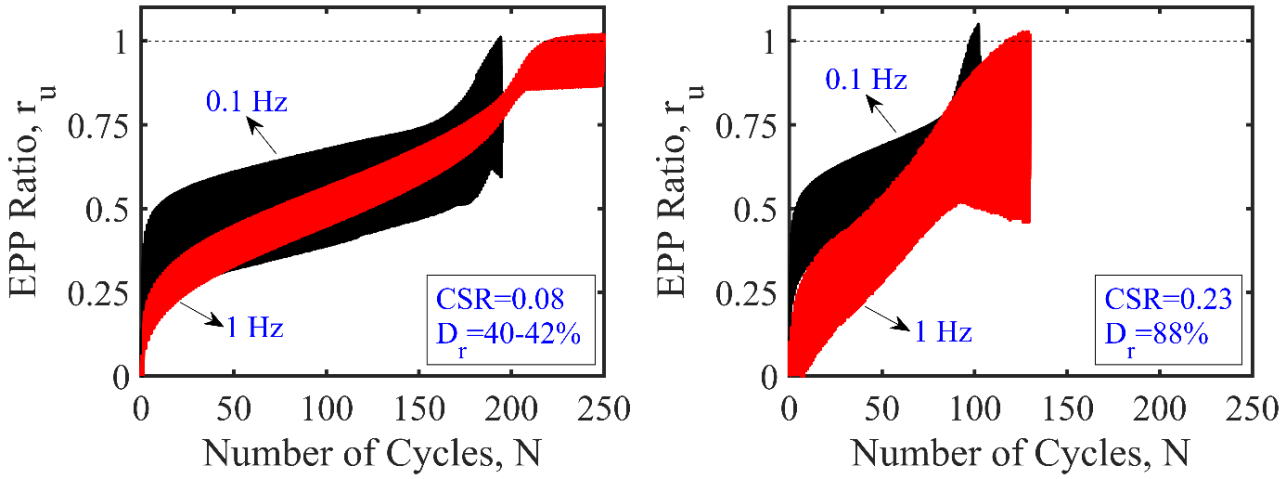

Figure 7. Typical excess pore pressure data recorded at different loading frequencies

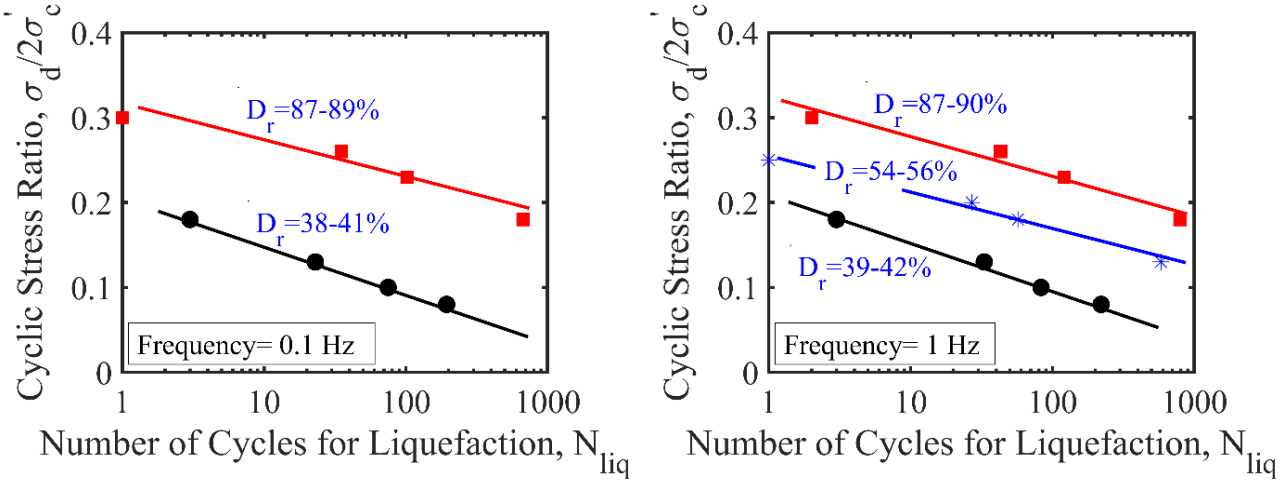

Figure 8. Influence of relative density on liquefaction resistance of sand

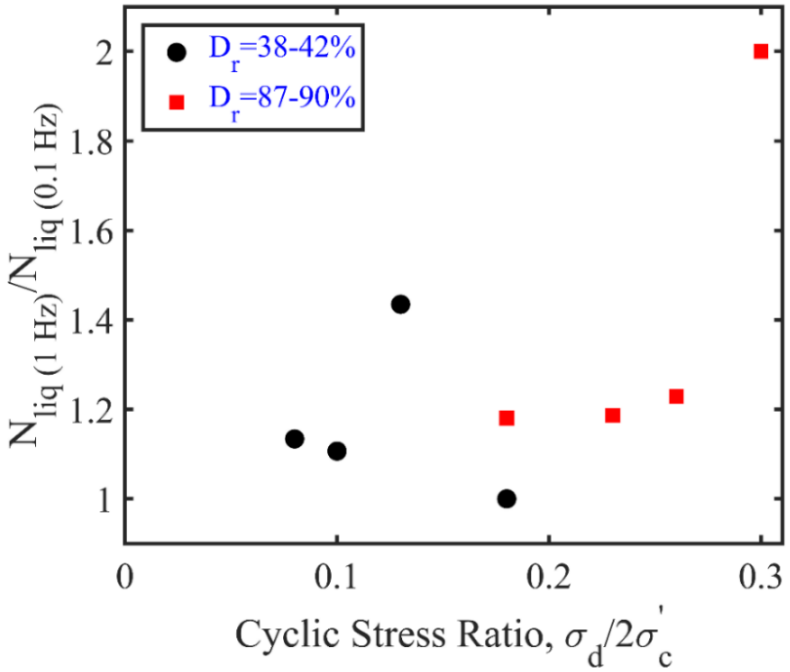

Figure 9. Influence of cyclic loading frequency on sand's liquefaction resistance

4. Conclusions

Earthquake-induced liquefaction is a complicated phenomenon. Over the years, significant research has been performed in the laboratory and/or field to improve the understanding of the liquefaction behavior of sandy soils. Despite an important amount of research effort, there are still important uncertainties and disagreements regarding some aspects of soil liquefaction. The role that some soil parameters and loading conditions play in the cyclic behavior of liquefiable soils has not been adequately understood, and the results of published studies are usually contradictory.

This work intends to provide insights into the liquefaction behavior of clean sand, paying particular attention to the impact of relative density and loading frequency on the excess pore pressure generation. With this aim, a total of 20 stress-controlled undrained dynamic triaxial experiments were conducted on saturated, clean sand specimens. The following conclusions are deduced from this work.

Under comparable test conditions (i.e., similar cyclic stress ratio and loading frequency), lower excess pore pressures were accumulated in dense specimens than in loose specimens, suggesting that the resistance of sand to liquefaction increases with an increase in relative density. These results seem to correlate well with the published studies.

Loading frequency was observed to influence the excess pore pressure behavior and liquefaction resistance of sand prepared at different relative densities. The resistance of sand to liquefaction tends to increase as the loading frequency is increased. This effect was more pronounced for dense specimens. In every case, excess pore pressures were generated faster at the early stages of the cyclic loading. The rate of excess pore pressure generation was greater at a lower frequency. These results highlight that the state of practice should appropriately account for the impacts of loading frequency to accurately assess the liquefaction behavior of sand.

This study incorporated the effects of two parameters only, and the test data was collected using a sinusoidal type of loading and effective confining stress of 100 kPa. Future tests should consider the other test parameters (i.e., stress level) and examine the combined effects of these parameters under various cyclic loading patterns that closely replicate the actual earthquake excitation.

Acknowledgment

The author thanks Murat ULU and Tahsin CALP for their technical assistance and support during the experiments.

Statement of Research and Publication Ethics

This study complies with scientific research and publication ethics and principles.

References

[1] I. Towhata, "Geotechnical Earthquake Engineering," Springer, 2008.
[2] M. Wyss and J. N. Brune, "The Alaska Earthquake of 28 march 1964: a complex multiple rupture," Bull. Seismol. Soc. Am., vol. 57, no. 5, pp. 1017-1023, Oct. 1967. [Online]. Available: https://authors.library.caltech.edu/48262/1/1017.full.pdf. [Accessed: Apr. 21, 2022].
[3] K. Ishihara and Y. Koga, "Case studies of liquefaction in the 1964 Niigata Earthquake," Soils Found., vol. 21, no. 3, pp. 35-52, Sep. 1981, doi: https://doi.org/10.3208/sandf1972.21.3_35
[4] K. Ishihara, F. Tatsuoka, and S. Yasuda, "Undrained deformation and liquefaction of sand under cyclic stresses," Soils Found., vol. 15, no. 1, pp. 29-44, Mar. 1975, doi: https://doi.org/10.3208/sandf1972.15.29
[5] F. H. Lee, "Centrifuge modelling of earthquake effects on sand embankments," Ph.D. dissertation, Dept. Civil Eng., Cambridge Univ., Cambridge, UK, 1985.
[6] T. L. Holzer, T. C. Hanks, and T. L. Youd, "Dynamics of liquefaction during the 1987 Superstition Hills, California, Earthquake," Science, vol. 244, no. 4900, pp. 56-59, Apr. 1989, doi: https://doi.org/10.1126/science.244.4900.56
[7] H. B. Seed and K. L. Lee, "Liquefaction of saturated sands during cyclic loading," J. Soil Mech. Found, vol. 92, no. 6, pp. 105-134, Nov. 1966, doi: https://doi.org/10.1061/JSFEAQ.0000913
[8] K. Ishihara, "Liquefaction and flow failure during earthquakes," Géotechnique, vol. 43, no. 3, pp. 351-451, Sep. 1993, doi: https://doi.org/10.1680/geot.1993.43.3.351
[9] B. Muhunthan and A. N. Schofield, "Liquefaction and dam failures," Slope Stability 2000, ASCE Special Publication, 266-280, Aug. 2000, doi: https://doi.org/10.1061/40512(289)20
[10] H. B. Seed and W. H. Peacock, "Test procedures for measuring soil liquefaction characteristics," J. Soil Mech. Found., vol. 97, no. 8, pp. 1099-1119, Aug. 1971, doi: https://doi.org/10.1061/JSFEAQ.0001649
[11] K. Ishihara, "Stability of natural deposits during earthquakes," in 11th Int. Conf. on Soil Mechanics and Foundation Engineering, Balkema, San Francisco, USA, Aug. 12-16, 1985, pp. 321-376. [Online]. Available: https://www.issmge.org/publications/publication/stability-of-natural-deposits-during-earthquakes. [Accessed: Apr. 21, 2022].
[12] W. Finn, R. Ledbetter, and G. Wu, "Liquefaction in silty soils: design and analysis. ground failures under seismic conditions," ASCE, pp. 51-76, 1994.

[13] S. Thevanayagam, M. Fiorillo, and J. Liang, "Effect of nonplastic fines on undrained cyclic strength of silty sands," Soil Dynamics and Liquefaction 2000, 77-91, 2000, doi: https://doi.org/10.1061/40520(295)6
[14] C. P. Polito and II J. R. Martin, "Effects of nonplastic fines on the liquefaction resistance of sands," J. Geotech. Geoenviron. Eng., vol. 127, no. 5, pp. 408-415, May 2001, doi: https://doi.org/10.1061/(ASCE)1090-0241(2001)127:5(408)
[15] D. D. Porcino and V. Diano, "The influence of non-plastic fines on pore water pressure generation and undrained shear strength of sand–silt mixtures," Soil Dyn. Earthq. Eng., vol. 101, pp. 311-321, Oct. 2017, doi: https://doi.org/10.1016/j.soildyn.2017.07.015
[16] E. E. Eseller-Bayat, M. Monkul, Ö. Akin, and S. Yenigun, "The coupled influence of relative density, CSR, plasticity and content of fines on cyclic liquefaction resistance of sands. J. Earthq. Eng., vol. 23, no. 6, pp. 909-929, 2019, doi: https://doi.org/10.1080/13632469.2017.1342297
[17] E. Karakan, N. Tanrinian, and A. Sezer, "Cyclic undrained behavior and post liquefaction settlement of a nonplastic silt," Soil Dyn. Earthq. Eng., vol. 120, pp. 214-227, May 2019, doi: https://doi.org/10.1016/j.soildyn.2019.01.040
[18] Y. P. Vaid and S. Sivathayalan, "Fundamental factors affecting liquefaction susceptibility of sands," Can. Geotech. J., vol. 37, no. 3, pp. 592-606, June 2000, doi: https://doi.org/10.1139/t00-040
[19] J. A. H. Carraro, P. Bandini, and R. Salgado, "Liquefaction resistance of clean and nonplastic silty sands based on cone penetration resistance," J. Earthq. Eng., vol. 129, no. 11, pp. 965-976, Nov. 2003, doi: https://doi.org/10.1061/(ASCE)1090-0241(2003)129:11(965)
[20] K. Adalier and A. Elgamal, "Liquefaction of over-consolidated sand: a centrifuge investigation, J. Earthq. Eng., vol. 9, no. 1, pp. 127-150, 2005, doi: https://doi.org/10.1080/13632460509350582
[21] C. Liu and J. Xu, "Experimental study on the effects of initial conditions on liquefaction of saturated and unsaturated sand, "Int. J. Geomech., vol. 15, no. 6, Dec. 2013, doi: https://doi.org/10.1061/(ASCE)GM.1943-5622.0000350
[22] Y. Vaid, J. Chern, and H. Tumi, "Confining pressure, grain angularity and liquefaction. J. Geotech. Geoenviron. Eng., vol. 111, no. 10, 1229-1235, Oct. 1985, doi: https://doi.org/10.1061/(ASCE)0733-9410(1985)111:10(1229)
[23] Y. Yoshimi and H. Oh-oka, "Influence of degree of shear stress reversal on the liquefaction potential of saturated sand," Soils Found., vol. 15, no. 3, pp. 27-40, Sep. 1975, doi: https://doi.org/10.3208/sandf1972.15.3_27
[24] F. Tatsuoka, S. Toki, S. Miura, H. Kato, M. Okamoto, S. Yamada, S. Yasuda, and F. Tanizawa, "Some factors affecting cyclic undrained triaxial strength of sand," Soils Found., 26 (3): 99-116, Sep. 1986, doi: https://doi.org/10.3208/sandf1972.26.3_99
[25] C.P. Polito, "The effects of non-plastic and plastic fines on the liquefaction of sandy soils," Ph.D. dissertation, Virginia Polytechnic Institute and State University, Blacksburg, VA, USA, 1999. [Online]. Available: https://vtechworks.lib.vt.edu/handle/10919/30243. [Accessed: Apr. 21, 2022].
[26] X. H. Wang and H. L. Zhou, "Study on dynamic steady state strength of sand soil liquefaction," J. Rock Mech. Geotech. Eng., vol. 22, pp. 96-102, 2003.
[27] K. L. Lee and J. A. Fitton, "Factors affecting the cyclic loading strength of soil," ASTM International, STP33637S: 71-95, 1969, doi: https://doi.org/10.1520/stp33637s
[28] N. Y. Chang, N. P. Hsieh, D. L. Samuelson, and M. Horita, "Effect of frequency on liquefaction potential of saturated Monterey no. o sand. in: computational methods and experimental measurements," Edited by Keramidas G.A., Brebbia C.A., Springer, Berlin, Heidelberg, pp. 433-446, 1982, doi: https://doi.org/10.1007/978-3-662-11353-0_34
[29] Y. Guo and L. He, "The influences of the vibration frequencies on liquefaction strength of saturated sands," Journal of Disaster Prevention and Mitigation Engineering, vol. 29, pp. 618-623, 2009.
[30] T. Feng and L. Zhang, "Experimental study on effect of vibration frequency on dynamic behaviors of saturated sands," J. Water Resour. Plan. Manag., vol. 11, pp. 11-14, 2013.
[31] S. Zhang, Y. F. Zhang, L. K. Zhang, and C. J. Liu, "Influence of confining pressure and vibration frequency on the liquefaction strength of the saturated gravel sand," Journal of Xinjiang Agricultural University, vol. 38, pp. 68-71, 2015.
[32] Z. Nong, S. Park, S. W. Jeong, and D. E. Lee, "Effect of cyclic loading frequency on liquefaction prediction of sand," Appl. Sci., vol. 10, no. 13, pp. 4502, June 2020, doi: https://doi.org/10.3390/app10134502

[33] J. P. Mulilis, C. K, Chan, and H. B. Seed, "The effects of method of sample preparation on the cyclic stress-strain behavior of sands (EERC report 75-18). Berkeley, CA, USA: University of California, 1975.
[34] H. K. Dash and T. G. Sithara, "Effect of frequency of cyclic loading on liquefaction and dynamic properties of saturated sand," Int. J. Geotech, vol. 10, 5, pp. 487-492, May 2016, doi: https://doi.org/10.1080/19386362.2016.1171951
[35] H. Tsuchida, "Prediction and countermeasure against liquefaction the liquefaction in sand deposits," In Abstract of the Seminar, Port and Harbour Research Institute, 3.1-3.33, 1970.
[36] A. Zeybek, "Suggested method of specimen preparation for triaxial tests on partially saturated sand," Geotech. Test. J., vol. 45, no. 2, 2022, doi: https://doi.org/10.1520/GTJ20210168
[37] E. E. Eseller-Bayat and D. B. Gulen, "Undrained dynamic response of partially saturated sands tested in a DSS-C device," J. Geotech. Geoenviron. Eng., vol. 146, no. 11, pp. 04020118, 2020, doi: https://doi.org/10.1061/(ASCE)GT.1943-5606.0002361